Supplementary Text

Manuscript Title: Tuning ion coordination architectures to enable selective partitioning.

Authors: Sameer Varma & Susan B. Rempe*
Computational Bioscience Department,
Sandia National Laboratories, Albuquerque, NM-87185, USA

****Corresponding Author:*** MS 0310, PO Box 5800, Albuquerque, NM 87185.
Email: slrempe@sandia.gov, Phone: (505) 845-0253, Fax: (505) 844-5670.

There are 9 sub-topics:

1. Methods – Implementation and simulation parameters in the quasi-chemical approach
2. Reaction free energies of ions in liquid formamide
3. Quasi-liquid environments of strongly selective K-channels
4. Reaction free energies of ions in quasi-liquid formamide
5. Reaction free energies of ions in quasi-liquid formamide without inter-ligand H-bonding
6. Components of the free energy for formation of 8-fold coordinated complexes
7. Distorted 5-fold coordinated complex of Na^+ ion formed from 4 glycine dipeptide ligands
8. Computation of K^+/Na^+ selectivity in figure 3(b)
9. Distorted 5-fold coordinated complex of K^+ ion formed from 4 glycine dipeptide ligands

1. Methods – Implementation and simulation parameters in the quasi-chemical approach

The statistical framework of the quasi-chemical theory for liquids is described in detail elsewhere (1-8). Here, we describe briefly the implementation protocol and provide all simulation parameters.

Consider the following reaction:

$$I^{+}_{gas} + n\left[X\right]_{M} \underset{\longleftarrow}{\overset{\Delta G_{I^{+}\rightarrow I^{+}(X)_{n}}(M)}{\longrightarrow}} \left[I^{+}X_{n}\right]_{M} \qquad [S1]$$

To assess the free energies $\left(\Delta G_{I^{+}\rightarrow I^{+}(X)_{n}}(M)\right)$ for these association reactions in the quasi-chemical setting, the region around an ion was divided into inner- and outer-shell domains. We define the inner-shell domain as the region containing the tighter subset of ligands directly coordinated to the ion. Since local interactions are most significant in differentiating the behavior of various ions binding to the same ligands, we treated the inner-shell interactions quantum mechanically; and the interactions with the remaining solvation phase beyond the inner coordination shell using an implicit solvent model. Note that a quantum mechanical treatment of local interactions has also been shown to be important in the context of K-channels (9).

The 3-dimensional structures of ligands (*X)* and their respective inner-shell coordination complexes with ions $\left(I^{+}(X)_{n}\right)$ were first optimized at the hybrid B3LYP (10-12) level of density functional theory (DFT). Each optimized structure was then utilized to determine its individual thermo-chemical properties via normal mode analysis at a temperature of 298.15 K and pressure of 1 atmosphere. All normal modes were found to be non-negative, therefore confirming the existence of energetically optimized structures. Next, these thermo-chemistries were combined to obtain gas-phase free energy changes for the various inner-shell coordination reactions, that is,

$$\Delta G_{I^{+}\rightarrow I^{+}(X)_{n}}(gas) = G_{I^{+}(X)_{n}}(gas) - G_{I^{+}}(gas) - n.G_{X}(gas) \qquad [S2]$$

Clearly, we assume in these computations an absence of anharmonicities. However, separate calculations demonstrate the presence of anharmonicity only in higher order (n>5) coordinations that contain inter-ligand hydrogen bonds, and that correction for these anharmonicities results in more exothermic association reactions, but without affecting any of the conclusions drawn in this work. The details of these calculations are not included here as they are the subject of a separate publication (Rempe, Leung & Varma, manuscript in preparation).

All optimization and subsequent frequency calculations were carried out with the *Gausssian 03* suite of programs (12) using the following basis sets: a 6-31G(d) basis set for Na^{+} ions, a 6-311+G(2d) basis set for K^{+} ions, a 6-31++G(d,p) basis set for the N, C, O & H atoms belonging to formamide molecules, and a 6-31G(d) basis set for the N, C,

O and H atoms belonging to glycine dipeptide molecules. Our reasons for selecting the basis sets for Na^+ and K^+ ions and formamide molecules emerge from a systematic exploration of several possibilities (13), and yield ion-water dissociation energies in excellent agreement with experiment (14). In a separate study (15), these basis sets were also found to reproduce accurately the gas-phase interactions of H_2O-H_2O and H_2O-HF dimers. The smaller basis set 6-31G(d) utilized to represent dipeptide glycine molecules was chosen for computational feasibility.

Next, the effect of the outer-shell solvation environment (*M*) surrounding both the complex and the free ligands was computed. This was done in two steps. Contributions computed in the first step and added on to the gas phase reaction free energies result in values that we refer to as quasi-liquid (*qL*) reaction free energies, that is,

$$\Delta G_{I^+ \to I^+(X)_n}(qL) = \Delta G_{I^+ \to I^+(X)_n}(gas) + \Delta G(gas \to qL) \qquad [S3]$$

This first step involves an implicit evaluation of the gain or loss in reaction free energy associated with higher or lower concentrations (or alternatively, higher or lower pressures), respectively, of ligands in relation to the gas phase. It is computed as:

$$\Delta G(gas \to qL) = -nRT \ln\left(C_{qL}/C_{gas}\right) \qquad [S4]$$

The concentration of formamide ligands in gas phase C_{gas} was taken as 0.041 M, while their concentration in liquid phase was taken as 25.2 M. The concentration of glycine dipeptide ligands in the selectivity filters of K-channels was taken as one half the concentration of carbonyl oxygens present in the selectivity filter of KcsA (16), and was computed to be 11.4 M. Note that the dependence of ligand concentrations on free energies is logarithmic, and therefore until concentrations of the ligands change by an order of magnitude, their effect on ion-ligand association free energies is negligible.

In the second step, the electrostatic energy for solvating a coordination complex in liquid phase is computed as,

$$\Delta G_{I^+(X)_n}(qL \to L) = \mu_{I^+(X)_n}(\varepsilon) - n.\mu_X(\varepsilon) \qquad [S5]$$

Here, $\mu_{I^+(X)_n}(\varepsilon)$ is the electrostatic stabilization of a coordination complex $I^+(X)_n$ by the liquid phase (dielectric constant, ε) outside the inner-shell, and $n.\mu_X(\varepsilon)$ is the electrostatic penalty associated with extracting *n* ligand molecules from the same phase outside the inner-shell. In practice, these electrostatic interactions of coordination complexes and ligands with the outer-domain can be computed using either implicit or explicit treatments of the outer-domain, and for monovalent cations, both treatments have been shown to reproduce results in excellent agreement with experiment (6). Here we compute these electrostatic interactions by treating the environment as an implicit solvent. Contributions computed in this step and added on to the quasi-liquid free energies result in liquid phase reaction free energies,

$$\Delta G_{I^+ \to I^+(X)_n}(L) = \Delta G_{I^+ \to I^+(X)_n}(qL) + \Delta G_{I^+(X)_n}(qL \to L) \qquad [S6]$$

Note that the calculation in the second step is required only to capture the effect of liquid phases that have dielectric constants greater than unity. Therefore, in this work, such a computation was carried out only to determine the reaction free energies of Na^+ and K^+ in liquid formamide (ε = 109.5). The finite difference scheme of the APBS package (17), with a finest grid spacing of 0.1 Å, was used for solving the Poisson's equation, the details of which can be found elsewhere (18). Partial charges of atoms in the ligands and complexes were obtained from separate DFT/B3LYP calculations using the optimized structures and the ChelpG method (19), and were distributed over the FD grids using cubic B-spline discretization; atomic radii required for defining solvent exclusion regions were taken from Stefanovich & Truong (20); the radius of formamide required for creating molecular surfaces on the FD grid was taken as 2.15 Å (21); and finally the radii needed to partition the aforementioned inner- and outer-shell domains were taken as 3.9 Å for both Na^+ and K^+ ions. Alternate choices explored for these radii were found to have only a small effect on the solvation energies of these ions.

2. Reaction free energies of ions in liquid formamide

Figure S1 illustrates the solvation free energies of K^+ and Na^+ ions in liquid formamide (NH_2CHO). We find that just like in liquid water, and in spite of the stronger electrostatic field strengths (or dipole moments) of formamide carbonyl ligands, both ions still prefer strong coordination with exactly 4 ligands. We also find that, consistent with experimental values (21-23), the solvation free energies of the ions are equivalent to their respective hydration free energies. In other words, neither the structural nor the energetic properties of the ions differ noticeably when partitioned from liquid water to liquid formamide.

Figure S1: Reaction free energies of K^+ & Na^+ ions in liquid formamide.

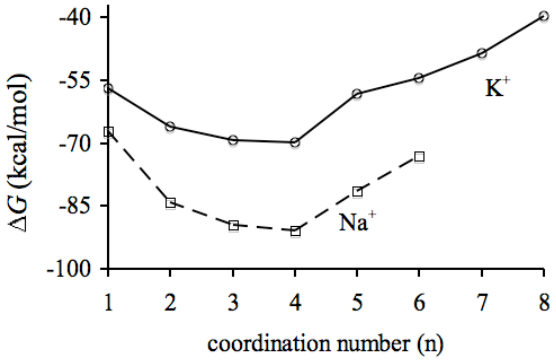

This finding appears quite surprising at first, but can be understood by considering the following. Consistent with the notion of formamide having a dipole moment (3.73 Debye) stronger than water (1.85 Debye), we find that ions do in fact bind more tightly to formamide ligands, but that occurs only in the gas phase and is apparent from a comparison of gas phase reaction free energies of the ions (figure S2). The nature of ion-ligand association is, however, different in liquid phase, as its computation in liquid phase also requires incorporation of the electrostatic penalties associated with extracting ligands from their respective liquid media. Because the dielectric constant of liquid formamide (109.5) is also greater than liquid water (78.5), which is not to be confused as being entirely a consequence of the stronger dipole moment of formamide molecules, the desolvation penalty associated with extracting a formamide molecule from liquid formamide (10.8 kcal/mol) is also higher than that of the desolvation penalty associated with extracting a water molecule from liquid water (8.4 kcal/mol). Therefore when ions are partitioned from liquid water to liquid formamide, these two effects, namely, the stronger ion-formamide interactions and the larger penalties for extracting formamide molecules from liquid phase, almost completely cancel each other out, and result in ion solvation characteristics similar to those in liquid water.

Figure S2: Reaction free energies of ions with water and formamide in gas phase.

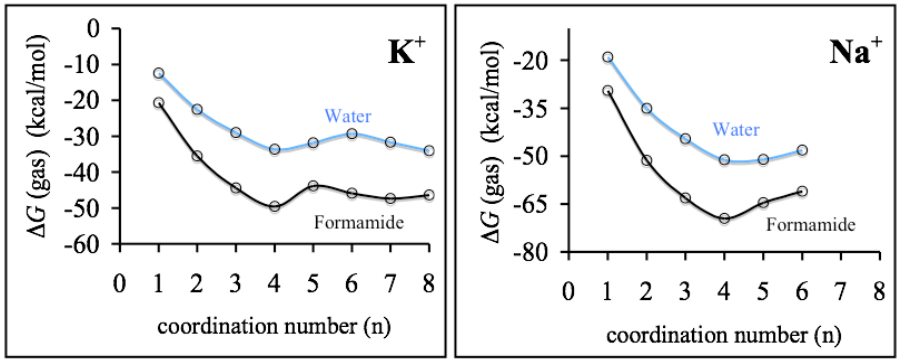

3. Quasi-liquid environments of strongly selective K-channels

Figure S3: Distribution of side-chain H-bond donors in strongly selective K-channels KcsA (24), KvAP (25), KirBac1.1 (26) and MthK (27). The orientation of each potassium channel is as viewed from its respective extra-cellular end. Channel backbones are illustrated as cartoons in yellow, while side chains of H-bond donor residues His, Arg, Lys, Gln, Asn, Trp, Tyr, Thr, Ser, and Cys are illustrated as sticks in blue. Pair-wise distance calculations between H-bond donor groups of these residues and ion-coordinating carbonyl oxygen atoms show that there are no relevant H-bond donor

groups within a direct coordination distance of 6 Å from the carbonyl oxygens. Each embedded illustration was created using PyMoL.

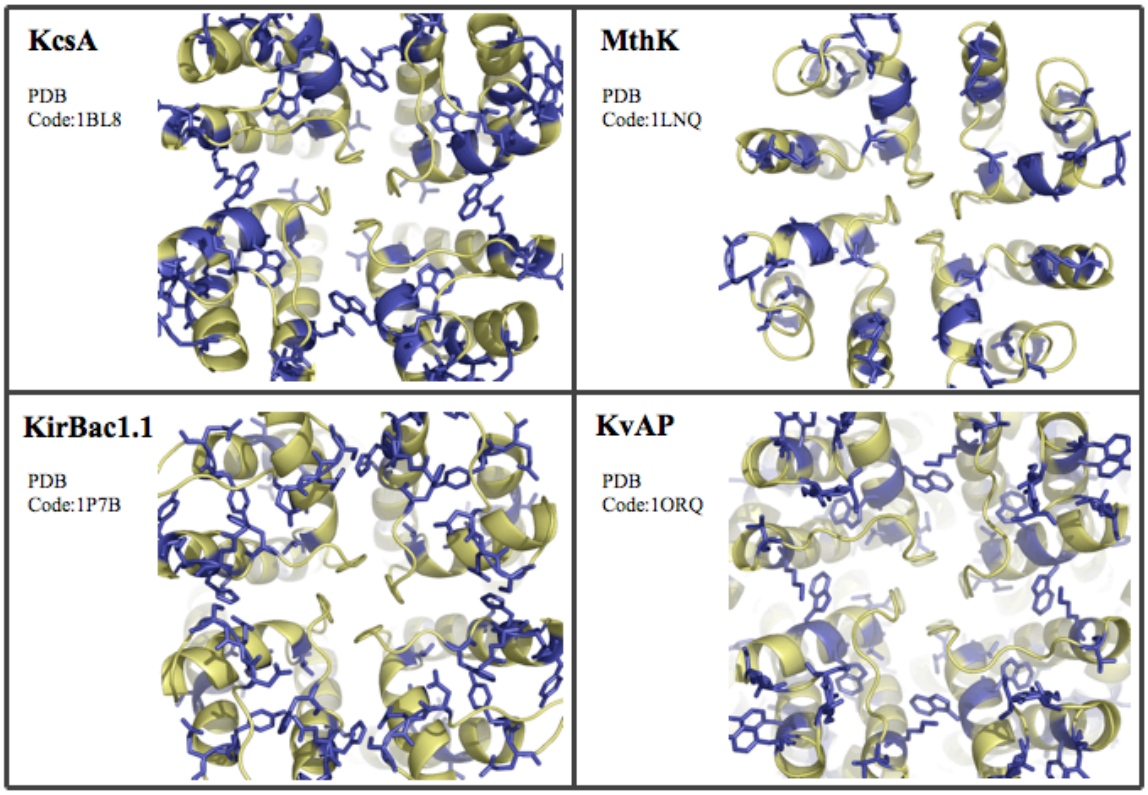

4. Reaction free energies of ions in quasi-liquid formamide

Figure S4: Reaction free energies of Na^+ and K^+ ions in quasi-liquid formamide.

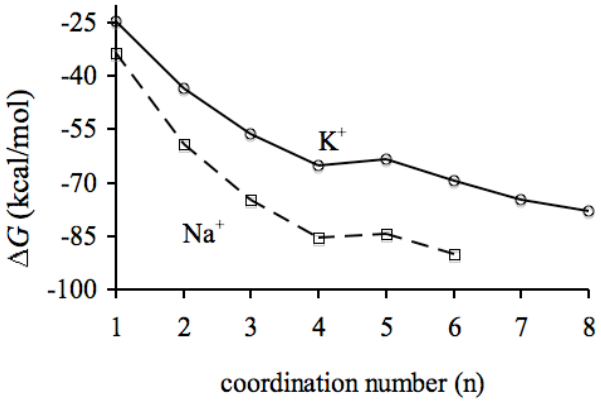

5. Reaction free energies of ions in quasi-liquid formamide without inter-ligand H-bonding

Table S1: Components of the free energy for formation of non-hydrogen bonded formamide complexes [$I^+(NH_2CHO)_n$] in gas (g) and quasi-liquid (qL) phases. $\Delta G(g)$ refers to the free energy in the gas phase (Equation S2); $\Delta G(qL)$ refers to the free energy in the quasi-liquid phase (Equation S3) after accounting for the difference between the concentrations of ligands in gas ($C(g)$ = 0.041 M) and liquid phase ($C(L)$ = 25.2 M). The concentration of carbonyl oxygens in the selectivity filters of K-channels was computed to be 22.8 M, similar to the concentration of formamide in liquid phase. All energies are in units of kcal/mol.

I^+	n	$\Delta G(g)$	$-nRT\ln\left(C(L)/C(g)\right)$	$\Delta G(qL)$
K^+	1	-20.7	-3.9	-24.6
	2	-35.5	-7.9	-43.4
	3	-44.4	-11.8	-56.2
	4	-49.6	-15.7	-65.3
	5	-43.5	-19.6	-63.2
	6	-39.8	-23.6	-63.4
	7	-36.7	-27.5	-64.2
	8	-29.3	-31.4	-60.7
Na^+	1	-29.4	-3.9	-33.4
	2	-51.3	-7.9	-59.2
	3	-63.1	-11.8	-74.9
	4	-69.5	-15.7	-85.2
	5	-64.6	-19.6	-84.2
	6	-61.0	-23.6	-84.6

6. Components of the free energy for formation of 8-fold coordinated complexes

Table S2: Components of the free energy for formation of 8-fold K^+ coordination complexes $[K^+X_n]_M$. ΔH refers to the change in enthalpy; $T\Delta S$ the change in entropy; and $\Delta G(qL)$ refers to the free energy change in the quasi-liquid phase after accounting for the difference between the concentrations of ligands in gas ($C(g)$) and condensed phases (C). The concentration of formamide was taken as 0.041 M in gas phase and 25.2 M in condensed phase. The concentration of glycine dipeptide molecules was taken as 0.041M in gas phase and 11.4 M in condensed phase. All energies are in units of kcal/mol.

Ligands (*X*)	***n***	ΔH	$-T\Delta S$ $(T = 298.15K)$	$-nRT\ln\left(C/C(g)\right)$	$\Delta G(qL)$
Formamide (H-bonded)	8	-127.6	81.2	-31.4	-77.8
Formamide (Not H-bonded)	8	-101.8	72.5	-31.4	-60.7
Glycine dipeptide	4	-107.3	50.8	-13.8	-70.3

7. Distorted 5-fold coordinated complex of Na^+ ion formed from 4 glycine dipeptide ligands

Attempts to optimize 4 bidentate ligands around a Na^+ ion quantum chemically (DFT/B3LYP), such that all of the 8 carbonyl oxygens directly coordinate the ion, fail. Instead an overall 5-fold coordinated structure results, with 3 oxygens pushed outside the ion's inner coordination shell, as illustrated in figure S5. This structure can also be described as a distorted K-channel binding site structure having an RMSD of 1.8 Å with respect to the x-ray coordinates of the S2 binding site of KcsA. The free energy to partition a Na^+ ion from liquid water into this structure is favorable by -9.5 kcal/mol, that is,

$$\Delta G_{Na^+ \to Na^+(GG)_4}(qL) - \Delta G_{Na^+ \to Na^+(H_2O)_4}(L) = -9.5 \text{ kcal/mol.}$$

Figure S5: Distorted 5-fold coordinated complex of Na^+ ion formed from 4 dipeptide glycine ligands. Na^+ is illustrated as a sphere, and the dipeptide glycine molecules are illustrated as sticks with carbons in green, oxygens in red, nitrogens in blue and hydrogens in white. The oxygens directly coordinating the Na^+ ion (average distance, 2.4 Å) are shown connected to it using dashed red lines; while the oxygens that are *not*

directly coordinating the Na^+ (average distance, 5.6 Å) are shown connected to it ion using dashed black lines.

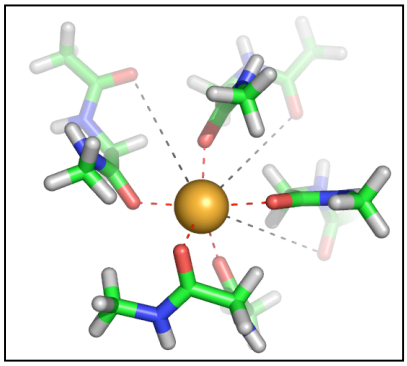

8. Computation of K^+/Na^+ selectivity in figure 3(b)

Figure 3(b) of the main text illustrates the electronic energy differences for transferring a Na^+ relative to a K^+ ion into different 8-fold glycine dipeptide (*GG*) geometries. These 8-fold geometries $\{(GG_i)_4\}$ were created by radial expansions or contractions of the 8-fold bidentate structure $(GG_o)_4$ optimized in the presence of a K^+ ion. The skewed cubic nature of the geometry was retained to keep all ligating oxygen atoms furthest away from each other. The positions of Na^+ ions relative to these geometries were then determined using quantum chemical (DFT/B3LYP) optimization. The positions of all atoms other than the ion were kept fixed during optimization to ensure direct 8-fold coordination, as otherwise a lower coordination structure results. Representative optimized geometries are illustrated in figure S6, along with a schematic of this procedure. The K^+/Na^+ selectivity for each geometry $(GG_i)_4$ was then calculated using the optimum position of the Na^+ ion as:

$$\begin{aligned}\Delta\Delta\Delta G^{electronic}_{Na^+(GG_i)_4 \rightarrow K^+(GG_o)_4} &= \Delta G^{electronic}_{K^+ \rightarrow K^+(GG_o)_4}(qL) - \Delta G^{electronic}_{K^+ \rightarrow K^+(H_2O)_4}(L) \\ &\quad -\Delta G^{electronic}_{Na^+ \rightarrow Na^+(GG_i)_4}(qL) + \Delta G^{electronic}_{Na^+ \rightarrow Na^+(H_2O)_4}\end{aligned} \qquad [S6]$$

Figure S6: Schematic for computation of K^+/Na^+ selectivity in figure 3(b) of main text, along with four representative 8-fold geometries, one around K^+ ion and three around Na^+ ions. The K^+ and Na^+ ions are drawn as small blue and green spheres, respectively, while the geometric center (GC) of the 8 coordinating oxygens in each configuration is represented as a small yellow sphere. As expected for cavity sizes comparable to or larger than those observed in the K-channel binding sites (28), the optimum positions of Na^+ ions do not coincide with the GC, but are displaced by distances indicated by $R_{I\text{-}GC}$. The

value of $R_{I\text{-}GC}$ approaches zero as the cavity size becomes smaller. The size of each cavity is represented as the distance between its furthest (diagonal) ligating oxygen atoms, $R_{O\text{-}O}$.

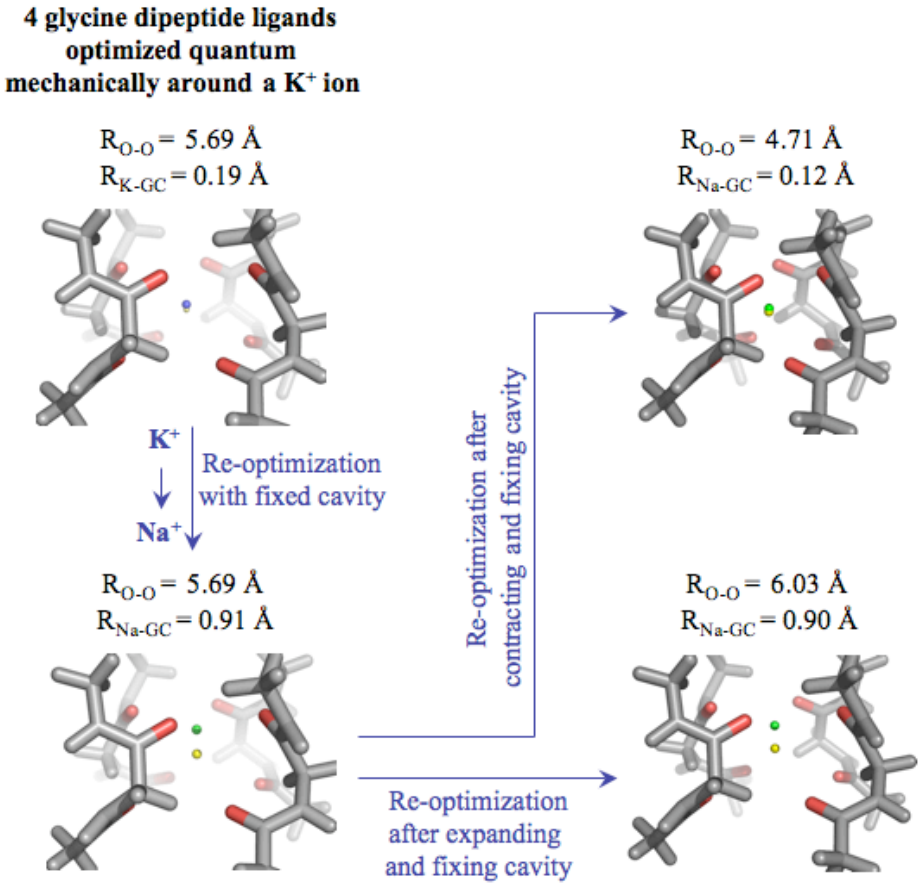

9. Distorted 5-fold coordinated complex of K^+ ion formed from 4 glycine dipeptide ligands

The Na^+ ion in the 5-fold coordinated structure illustrated in figure S5 was substituted with a K^+ ion, and the structure was re-optimized using quantum chemistry (DFT/B3LYP). The resulting optimum 5-fold coordinated structure with a K^+ ion is illustrated in figure S7. The free energy to partition a K^+ ion from liquid water into this structure is favorable by -10.1 kcal/mol, that is,

$$\Delta G_{K^+ \to K^+(GG)_4}(qL) - \Delta G_{K^+ \to K^+(H_2O)_4}(L) = -10.1 \quad \text{kcal/mol.}$$

Figure S7: Distorted 5-fold coordinated complex of K^+ ion formed from 4 dipeptide glycine ligands. K^+ is illustrated as a sphere, and the dipeptide glycine molecules are illustrated as sticks with carbons in green, oxygens in red, nitrogens in blue and hydrogens in white. The oxygens directly coordinating the K^+ ion (average distance, 2.7 Å) are shown connected to it using dashed red lines; while the oxygens that are *not* directly coordinating the K^+ (average distance, 5.9 Å) are shown connected to it ion using dashed black lines.

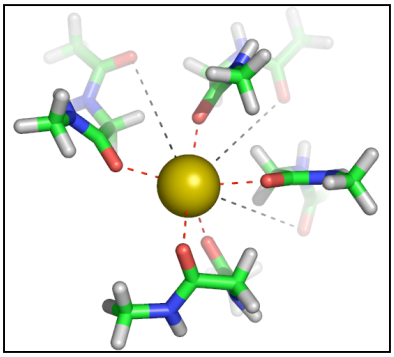

Supplementary References

1. Widom, B. 1982. Potential-Distribution Theory and the Statistical Mechanics of Fluids. J Phys. Chem. 86:869-872.

2. Pratt, L. R. and R. A. LaViolette. 1998. Quasi-chemical Theories of Associated Liquids. Mol. Phys. 95:909-915.

3. Martin, R. L., P. J. Hay, and L. R. Pratt. 1998. Hydrolysis of Ferric Ion in Water and Conformational Equilibrium. J Phys. Chem. A 102:3565-3573.

4. Pratt, L. R. and S. B. Rempe. Quasi-Chemical Theory and Implicit Solvent Models for Simulations. In: L. R. Pratt and G. Hummer, editors; 1999. p 172-201.

5. Rempe, S. B. and L. R. Pratt. 2001. The hydration number of Na^+ in liquid water. Fluid Phase Equilibria 183:121-132.

6. Asthagiri, D., L. R. Pratt, and H. S. Ashbaugh. 2003. Absolute hydration free energies of ions, ion–water clusters, and quasichemical theory. J Chem. Phys. 119:2702-2708.

7. Asthagiri, D., L. R. Pratt, M. E. Paulaitis, and S. B. Rempe. 2004. Hydration Structure and Free Energy of Biomolecularly Specific Aqueous Dications, Including Zn^{2+} and First Transition Row Metals. J. Amer. Chem. Soc. 126:1285-1289.

8. Beck, T. L., M. E. Paulaitis, and L. R. Pratt. 2006. The Potential Distribution Theorem and Models of Molecular Solutions. New York: Cambridge University Press. p. 244.

9. Bucher, D., S. Raugei, L. Guidoni, M. D. Peraro, U. Rothlisberger, P. Carloni, and M. L. Klein. 2006. Polarization effects and charge transfer in the KcsA potassium channel. Biophys. Chem. 124:292-301.

10. Becke, A. D. 1993. Density-functional thermochemistry. III. The role of exact exchange. J Chem. Phys. 98:5648-5652.

11. Lee, C., W. Yang, and R. G. Parr. 1988. Development of the Colle-Salvetti correlation-energy formula into a functional of the electron density. Phys. Rev. B 37:785-789.

12. Frisch, M. J., G. W. Trucks, H. B. Schlegel, G. E. Scuseria, M. A. Robb, J. R. Cheeseman, J. Montgomery, J. A., T. Vreven, K. N. Kudin, J. C. Burant, J. M. Millam, S. S. Iyengar, J. Tomasi, V. Barone, B. Mennucci, M. Cossi, G. Scalmani, N. Rega, G. A. Petersson, H. Nakatsuji, M. Hada, M. Ehara, K. Toyota, R. Fukuda, J. Hasegawa, M. Ishida, T. Nakajima, Y. Honda, O. Kitao, H. Nakai, M. Klene, X. Li, J. E. Knox, H. P. Hratchian, J. B. Cross, V. Bakken, C. Adamo, J. Jaramillo, R. Gomperts, R. E. Stratmann, O. Yazyev, A. J. Austin, R. Cammi, C. Pomelli, J. W. Ochterski, P. Y. Ayala, K. Morokuma, G. A. Voth, P. Salvador, J. J. Dannenberg, V. G. Zakrzewski, S. Dapprich, A. D. Daniels, M. C. Strain, O. Farkas, D. K. Malick, A. D. Rabuck, K. Raghavachari, J. B. Foresman, J. V. Ortiz, Q. Cui, A. G. Baboul, S. Clifford, J. Cioslowski, B. B. Stefanov, G. Liu, A. Liashenko, P. Piskorz, I. Komaromi, R. L. Martin, D. J. Fox, T. Keith, M. A. Al-Laham, C. Y. Peng, A. Nanayakkara, M. Challacombe, P. M. W. Gill, B. Johnson, W. Chen, M. W. Wong, C. Gonzalez, and J. A. Pople. 2004. Gaussian 03. Gaussian, Inc., Wallingford CT.

13. Varma, S. and S. B. Rempe. 2007. Can solvation phase properties increase coordination preferences of ions? Submitted.

14. Blades, A. T., J. S. Klassen, and P. Kebarle. 1996. Determination of Ion-Solvent Equilibria in the Gas Phase. Hydration of Diprotonated Diamines and Bis(trimethylammonium) Alkanes. J. Amer. Chem. Soc. 118:12437-12442.

15. Salvador, P., B. Paizs, M. Duran, and S. Suhai. 2001. On the effect of the BSSE on Intermolecular Potential Energy Surfaces. Comparison of a priori and a posteriori BSSE correction schemes. J Comp. Chem. 22:765-786.

16. Zhou, Y., J. H. Morais-Cabral, A. Kaufman, and R. MacKinnon. 2001. Chemistry of ion coordination and hydration revealed by a K^+ channel-Fab complex at 2.0 A resolution. Nature. 414:43-48.

17. Baker, A. N., D. Sept, S. Joseph, M. Holst, and A. J. McCammon. 2001. Electrostatics of nanosystems: Application to microtubules and the ribosome. Proc. Natl. Acad. Sci. USA. 98:10037-10041.

18. Varma, S. and E. Jakobsson. 2004. Ionization states of residues in OmpF and Mutants: Effects of Dielectric Constant & Interactions between Residues. Biophys. J. 86:690-704.

19. Breneman, C. M. and K. B. Wiberg. 1990. Determining Atom-Centered Monopoles from Molecular Electrostatic Potentials. The Need for High Sampling Density in Formamide Conformational Analysis. J Comp. Chem. 11:361-373.

20. Stefanovich, E. V. and T. N. Truong. 1995. Optimized Atomic Radii for Quantum Dielectric Continuum Solvation Models. Chem. Phys. Lett. 244:65-74.

21. Grossfield, A., P. Ren, and J. W. Ponder. 2003. Ion solvation thermodynamics from simulation with a polarizable force field. J Amer. Chem. Soc. 125:15671-15682.

22. Schmid, R., A. M. Miah, and V. N. Sapunov. 2000. A new table of tghe thermodynamic quantities of ion hydration. Phys. Chem. Chem. Phys. 2:97-102.

23. Cox, B. G. and A. J. Parker. 1973. Solvation of ions: XVII. Free energies, heats, and entropies of transfer of single ions from protic to dipolar aprotic solvents. J Amer. Chem. Soc. 95:402-407.

24. Doyle, D. A., J. M. Cabral, R. A. Pfuetzner, A. L. Kuo, J. M. Gulbis, S. L. Cohen, B. T. Chait, and R. MacKinnon. 1998. The structure of the potassium channel: molecular basis of K^+ conduction and selectivity. Science. 280:69-77.

25. Jiang, Y., A. Lee, J. Chen, V. Ruta, M. Cadene, B. T. Chait, and R. MacKinnon. 2003. X-ray structure of a voltage-dependent K^+ channel. Nature. 423:33-41.

26. Kuo, A., J. M. Gulbis, J. F. Antcliff, T. Rahman, E. D. Lowe, J. Zimmer, J. Cuthbertson, F. M. Ashcroft, T. Ezaki, and D. A. Doyle. 2003. Crystal structure of the potassium channel KirBac1.1 in the closed state. Science. 300:1922-1926.

27. Jiang, Y., A. Lee, J. Chen, M. Cadene, B. T. Chait, and R. MacKinnon. 2002. The open pore conformation of potassium channels. Nature. 417:523-526.

28. Bezanilla, F. and C. M. Armstrong. 1972. Negative Conductance Caused by Entry of Sodium and Cesium Ions into the Potassium Channels of Squid Axons J Gen. Physiol. 60:588-608.